frontiers in Materials

ORIGINAL RESEARCH
published: 09 March 2022
doi: 10.3389/fmats.2022.827009

Grapefruit Oil and Cobalt Nitrate-Loaded Polyurethane Hybrid Nanofibrous Scaffold for Biomedical Applications

Mohan Prasath Mani[1], *Ahmad Athif Mohd Faudzi*[2,3], *Shahrol Mohamaddan*[4], *Ahmad Fauzi Ismail*[5], *Rajasekar Rathanasamy*[6], *Manikandan Ayyar*[7] *and Saravana Kumar Jaganathan*[2,3,8]*

[1]School of Biomedical Engineering and Health Sciences, Faculty of Engineering, Universiti Teknologi Malaysia, Skudai, Malaysia, [2]Centre for Artificial Intelligence and Robotics, Universiti Teknologi Malaysia, Kuala Lumpur, Malaysia, [3]School of Electrical Engineering, Faculty of Engineering, Universiti Teknologi Malaysia, Johor Bahru, Malaysia, [4]Department of Bioscience and Engineering, College of Systems Engineering and Science, Shibaura Institute of Technology, Saitama, Japan, [5]Advanced Membrane Technology Research Centre (AMTEC), School of Chemical and Energy Engineering, Universiti Teknologi Malaysia, Skudai, Malaysia, [6]Department of Mechanical Engineering, Kongu Engineering College, Erode, India, [7]Department of Chemistry, Bharath Institute of Higher Education and Research (BIHER), Chennai, India, [8]Department of Engineering, Faculty of Science and Engineering, University of Hull, Hull, United Kingdom

OPEN ACCESS

Edited by:
Hem Raj Pant,
Tribhuvan University, Nepal

Reviewed by:
Kapil D. Patel,
Korea University, South Korea
Deval Prasad Bhattarai,
Tribhuvan University, Nepal

***Correspondence:**
Saravana Kumar Jaganathan
s.k.jaganathan@hull.ac.uk

Specialty section:
This article was submitted to Biomaterials, a section of the journal Frontiers in Materials

Received: *01 December 2021*
Accepted: *25 January 2022*
Published: *09 March 2022*

Citation:
Mani MP, Mohd Faudzi AA, Mohamaddan S, Ismail AF, Rathanasamy R, Ayyar M and Jaganathan SK (2022) Grapefruit Oil and Cobalt Nitrate-Loaded Polyurethane Hybrid Nanofibrous Scaffold for Biomedical Applications. Front. Mater. 9:827009. doi: 10.3389/fmats.2022.827009

The goal of this work is to fabricate a new composite based on polyurethane (PU), grapefruit (GP) oil, and cobalt nitrate [$Co(NO_3)_2$] using an electrospinning technique. Morphology results revealed the reduction in the fiber diameter of the composites compared to pristine PU control. The interaction of PU with GP and $Co(NO_3)_2$ was confirmed by hydrogen bond formation evident in infrared analysis. The fabricated PU/GP composites depicted a more hydrophobic behavior, while PU/GP/$Co(NO_3)_2$ showed a hydrophilic behavior than the pristine PU. Atomic force micrographs (AFM) revealed that the developed composites showed a decrease in the surface roughness (R_a) compared to PU. The addition of GP and $Co(NO_3)_2$ improved the mechanical strength of the pristine PU. The blood compatibility assays concluded not only the increase in blood clotting levels but also the less toxic nature of the fabricated composites compared to the pristine PU. Hence, the newly designed composites possessing outstanding physicochemical and biological properties may be used as a potential candidate for scaffolding in tissue engineering applications.

Keywords: PU, Co(NO3)2, grapefruit oil, electrospun scaffold, tissue engineering

INTRODUCTION

Tissue engineering is an emerging technique used for the recovering of the lost functions of the human tissue. This technique utilizes a natural/synthetic structure named "scaffold," which plays a key role in remodeling the damaged human tissue. The scaffold was combined with cell binding sites and growth factors in order to mimic the native extra cellular matrix (ECM) structure of the human tissue to support the cell proliferation, migration, and differentiation (Teixeira et al., 2020). The important characteristics of an ideal scaffold are its non-toxic, non-allergenic, biocompatible, and biodegradable nature (Zennifer et al., 2021). Recently, a scaffold based on a nanofibrous material was widely investigated in tissue engineering applications.

The various methods used for developing the nanofibers are freeze drying, particle leaching, solvent casting, self-assembly, gas foaming, electrospinning, phase separation, etc. (Li et al., 2018; Eltom et al., 2019). Nanofibers developed using some of the above techniques were found unfit for the wound healing applications owing to their large diameters and porous structure (Ali et al., 2016). However, the nanofibers based on the electrospinning technique provide adjustable pore size and surface area-to-volume ratios, which could have the ability to resemble the native ECM structure of human tissue (Vasita and Katti 2006; Liu et al., 2013; Wang et al., 2013). Further, the electrospun nanofibers also enhance the cell adhesion and proliferation and support the new tissue formation (Wang et al., 2013).

In tissue engineering applications, the polymeric materials (both natural and synthetic) were widely used for fabricating scaffolds. The natural polymers were chitosan, collagen, and silk fibroin, and synthetic polymers like polyvinyl alcohol (PVA), polylactide acid (PLA), polyurethane (PU), and poly (e-caprolactone) (PCL) were widely sought (Cui et al., 2010; Li et al., 2018). In this study, PU was used to develop nanofibers, and it was selected because of its desirable characteristics such as biocompatibility, biodegradability, and good oxidation stability (Polymer, 2019; Shen et al., 2015). Furthermore, literature showed that the scaffold based on polyurethane has widespread tissue engineering applications (Unnithan et al., 2012; Kuo et al., 2014; Tetteh et al., 2014; Subramaniam et al., 2018). Several modification strategies have been investigated in order to improve the physicochemical and biological properties of PU for tissue engineering applications. To state, Singh et al. (2020) modified PU with graphene oxide (GO) and hydroxyapatite (Hap) to serve as a scaffold for bone tissue engineering. The developed PU-GO/Hap composite showed improved thermal stability, better antimicrobial activity, and biocompatibility for U2OS cell growth. In another study, Almasian et al. (2020) developed a scaffold based on PU containing carboxymethyl cellulose (CC) and *Malva sylvestris* (MS) extract for wound healing applications. The fabricated PU/CC/MS composites showed satisfactory antimicrobial effects and improved the wound healing rate. Another interesting work from Kim et al. (2014) portrayed the significance of PU scaffold loaded with propolis for biomedical applications. Recently, Pant et al. (2015) fabricated a PU scaffold containing GO for stent coating. The developed PU/GO composite scaffold showed improved mechanical properties, hydrophilicity, and enhanced stability suitable for the stent coating.

In this study, PU was incorporated with grapefruit oil (GP) and cobalt nitrate [$Co(NO_3)_2$] in order to enhance their biological properties. The essential oil (EO) was obtained from the peel of grapefruit (*Citrus Paradisi. L*) through solvent-free microwave extraction and hydro-distillation. Grapefruit oil possesses almost 25 components. The dominant one among them is limonene (88.6%–91.5%) and some other constituents like β-pinene (0.8%–1.2%), linalool (1.1%–0.7%), and α-terpinene (0.7%–1.0%). Grapefruit EO stimulates body cleansing and removal of excess fluids (Uysal et al., 2011). GP has been reported to possess antibacterial and antigenotoxic effects (Cristóbal-Luna et al., 2018). The cobalt-incorporated materials were reported to be a hypoxia-mimicking material, which helps in activating the angiogenesis-related genes by artificial stabilization of hypoxia-inducible factor 1 (HIF-1). Few studies have reported the potential beneficial effects of cobalt (Co^{2+}) ions promoting angiogenesis. For instance, it was found that subcutaneous injections of cobalt in a rat kidney model promoted angiogenesis by activation of HIF-1. Furthermore, in a rat bladder *in vivo* model, cobalt stimulated the HIF-1α expression and vascular endothelial growth factor (VEGF), which ultimately influences the responses of hypoxia, cell growth, and angiogenesis (Hoppe et al., 2014). This study examines a new wound dressing scaffold based on polyurethane added with grapefruit oil and cobalt nitrate. After the electrospinning process, their physicochemical and biological properties were investigated to validate its feasibility.

MATERIALS AND METHODOLOGY

Materials

Tecoflex EG-80A with a molecular weight of 1,000 g/mol was used to fabricate electrospun scaffold. The grapefruit oil was obtained from a local market. Cobalt nitrate was procured from Sigma Aldrich, United Kingdom. The solvent dimethylformamide (DMF) was obtained from Merck, United States. The reagents used in partial thromboplastin time (APTT) and prothrombin time (PT) assay were obtained from Thermo Fisher Scientific, Selangor, Malaysia.

Preparation of Composite

To prepare a polymeric solution, PU of 9 wt% was prepared by dissolving in DMF and stirring overnight. The homogeneous solution of grapefruit oil (4 *w*/*v*%) and cobalt nitrate (4 wt%) was prepared by dissolving them in DMF and stirring for 1 h minimum. Finally, the composite solution is done by mixing a prepared homogeneous solution of PU, grapefruit oil, and cobalt nitrate at a ratio of 8:1 (*v*/*v*) and 8:0.5:0.5 (*v*/*v*) to make PU/GP and PU/GP/$Co(NO_3)_2$, respectively.

Fabrication of PU and Composite Scaffold

The scaffold of PU, PU/GP, and PU/GP/$Co(NO_3)_2$ composite was prepared by the electrospinning technique. In our study, the scaffold was prepared at a flow rate of 0.2 ml/h with a supply voltage of 10.5 kV. The distance from needle to collector drum was set as 20 cm.

Field Emission Scanning Electron Microscopy Micrographs

A field emission scanning electron microscopy (FESEM) unit was used for the morphology study of the electrospun PU, PU/GP, and PU/GP/$Co(NO_3)_2$ composites. The blank samples were gold coated and placed on the sample base of the FESEM. All the samples were captured and the fiber analyzed using ImageJ (National Institutes of Health, Bethesda, MD, United States) software to calculate the average fiber diameter.

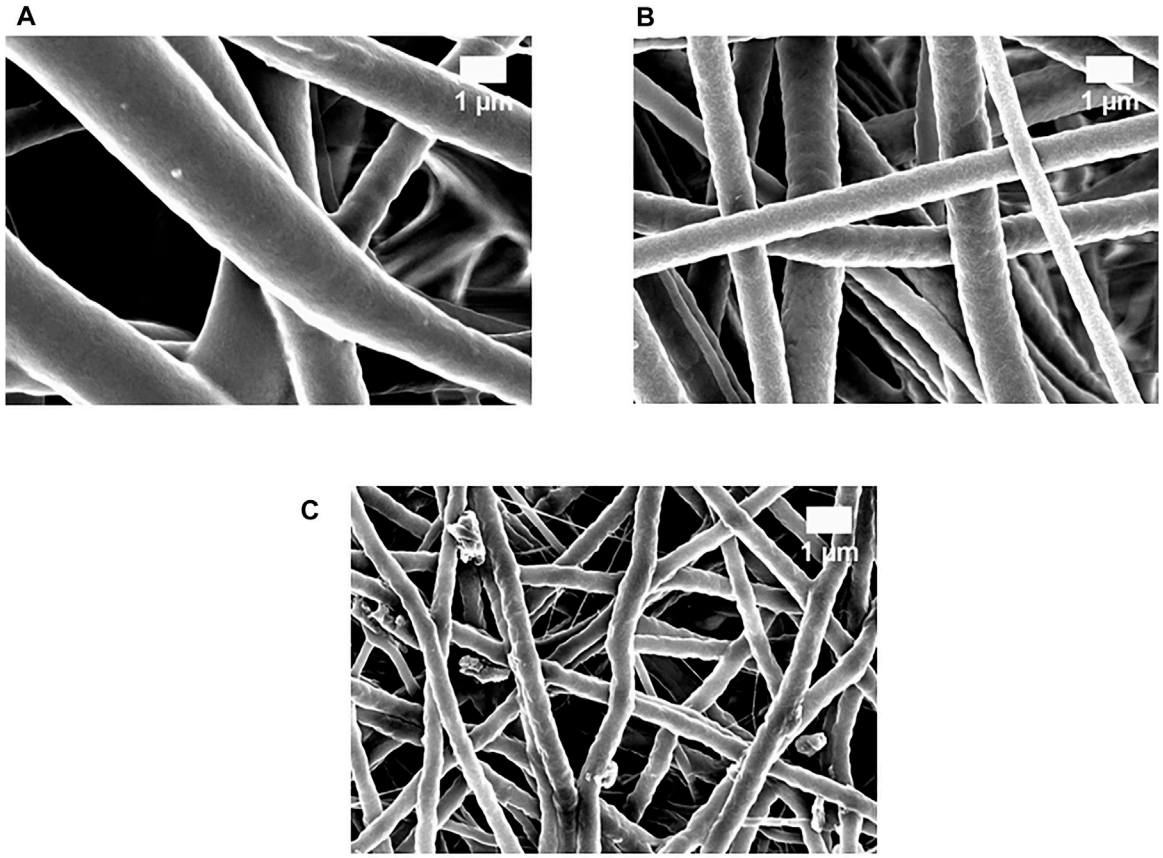

FIGURE 1 | Field emission scanning electron microscopy (FESEM) images of **(A)** polyurethane (PU), **(B)** PU/grapefruit (GP), and **(C)** PU/GP/cobalt nitrate [$Co(NO_3)_2$].

Fourier Transform Infrared Spectroscopy Analysis

The evaluation of chemical groups in the electrospun PU, PU/GP, and PU/GP/$Co(NO_3)_2$ composites was analyzed with an FTIR unit. For all samples, the spectrum in the range 600–4,000 cm^{-1} was scanned and recorded.

Contact Angle Measurements

To study the wetting behavior of electrospun PU, PU/GP, and PU/GP/$Co(NO_3)_2$ composites, the optima contact angle measurement unit was used. A small piece of web ($1 \times 5\ cm^2$) was fixed, and a drop of water from the needle was placed on the scaffold. An image of the droplet was captured using a high-resolution camera, and the angle of the droplet was calculated.

Thermogravimetric Analysis

TGA was performed for electrospun PU, PU/GP, and PU/GP/$Co(NO_3)_2$ composites under a Perkin Elmer thermal system. The experiment was done in nitrogen atmosphere, and the scans were done in the temperature range of 30°C–1,000°C with a heating rate of 10°C/min.

Atomic Force Microscopy

The average surface roughness of the developed scaffolds was estimated from the atomic force microscopy that was used. The experiment was done in the normal atmosphere at room temperature. Atomic force micrograph (AFM) images were taken in size of $20\ \mu m \times 20\ \mu m$ with 512×512 pixels, respectively.

Mechanical Testing

The mechanical strength of electrospun scaffolds was examined under a uniaxial testing machine. The tensile test was performed under a gauge length and cross head speed of 20 and 10 mm/min, respectively. From the stress strain plot, the maximum tensile strength was calculated and expressed in megapascals.

Blood Compatibility Measurements

The assays such as APTT, PT, and hemolysis were done to determine the blood compatibility nature of the electrospun scaffolds. The procedure for each analysis was based on the protocol as discussed previously in literature (Balaji et al., 2016).

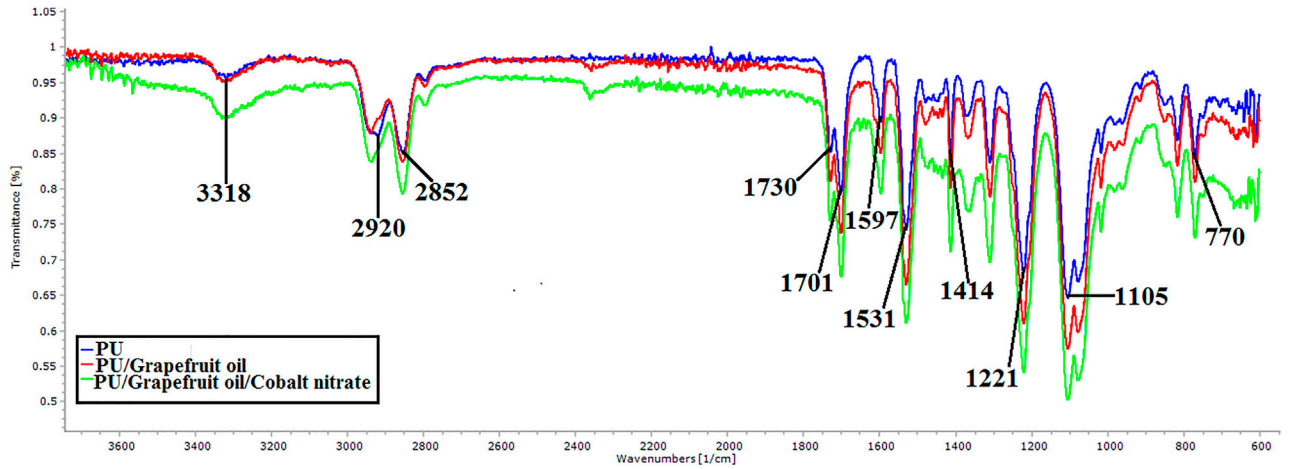

FIGURE 2 | FTIR curve of PU, PU/GP, and PU/GP/$Co(NO_3)_2$.

Statistical Analysis

All tests were performed in triplicate. One-way analysis of variance (ANOVA) was carried out, and the mean ± SD are obtained for all cases.

RESULTS

FESEM Analysis

Figure 1 shows the FESEM figures of the prepared electrospun scaffolds. It was observed that the as-spun nanofibrous scaffolds displayed a smoother and bead-less morphology with a non-woven structure. The average fiber diameter for pure PU was reported to be 1,513 ± 134 nm, while the PU/GP and PU/GP/$Co(NO_3)_2$ exhibited an average diameter of 967 ± 155 nm and 469 ± 157 nm, respectively. Furthermore, an EDS study confirmed the presence of cobalt in the polyurethane matrix. The polyurethane matrix showed an 8.1% weight of cobalt in addition to the carbon and oxygen content.

FTIR Analysis

FTIR spectra of the electrospun scaffolds were used to evaluate their chemical composition, and the spectra are indicated in **Figure 2**. In PU, a peak at 3,318 cm^{-1} denotes NH stretch, peaks at 2,920 and 2,852 cm^{-1} represent the CH stretch, and twin peaks seen at 1730 and 1701 cm^{-1} correspond to the CO group. Peaks at 1,531 and 1,597 cm^{-1} indicate the vibration of the NH group; the peak at 1,414 cm^{-1} corresponds to the CH vibrations; and the peaks at 1,221, 1,105, and 770 cm^{-1} represent the CO group with respect to alcohol (Balaji et al., 2016). There is no new peak formation for the developed nanocomposite scaffolds, but the PU peak intensity was altered (increased) with the addition of GP and $Co(NO_3)_2$. Further CH peak shift was also observed in which the peak at 2,920 cm^{-1} in PU was shifted to 2,941 cm^{-1} in PU/GP and 2,937 cm^{-1} in PU/GP/$Co(NO_3)_2$, respectively (Tijing et al., 2012).

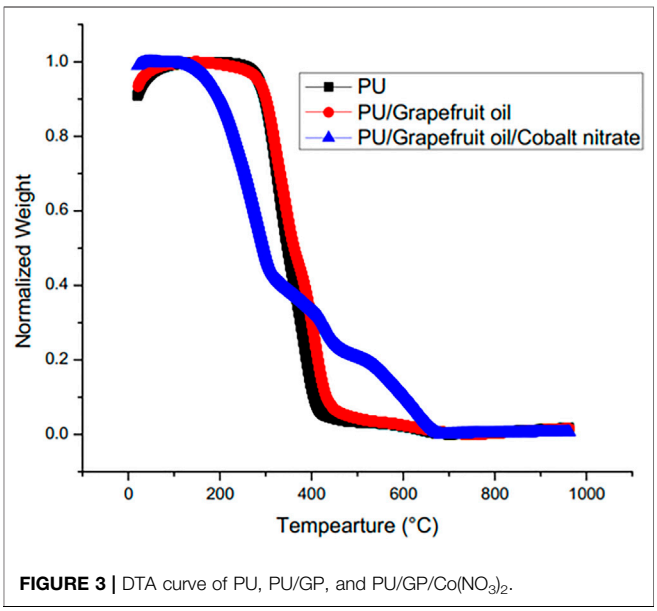

FIGURE 3 | DTA curve of PU, PU/GP, and PU/GP/$Co(NO_3)_2$.

Contact Angle Measurements

The static contact angle of pure PU scaffold was found to be 105° ± 3° while the PU containing GP and GP/$Co(NO_3)_2$ showed a contact angle of 109° ± 1° and 73° ± 1°, respectively.

Thermal Analysis

Figure 3 depicts the DTA curves of electrospun PU, PU/GP, and PU/GP/$Co(NO_3)_2$. From the DTA curve, the PU showed the initial degradation temperature at 284°C, while that temperature was increased to 290°C in electrospun PU/GP and decreased to 173°C in PU/GP/$Co(NO_3)_2$. Furthermore, DTG for the electrospun scaffolds is shown in **Figure 4**, and it was inferred that all electrospun scaffolds displayed three weight loss peaks. In PU weight loss curve, the first loss was seen from 222°C to 360°C, the second loss from 360°C to 517°C, and the third loss from

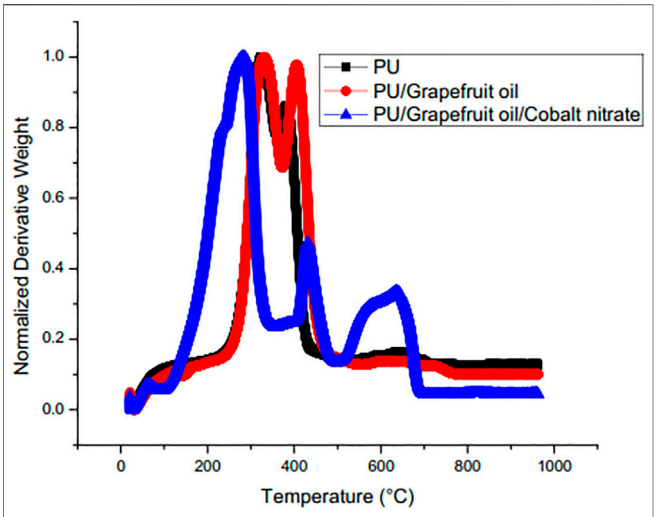

FIGURE 4 | DTG curve of PU, PU/GP, and PU/GP/$Co(NO_3)_2$.

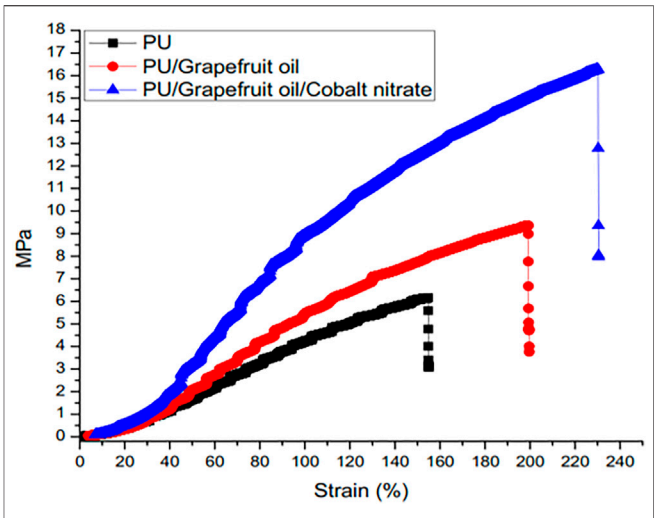

FIGURE 6 | Tensile curves of PU, PU/GP, and PU/GP/$Co(NO_3)_2$.

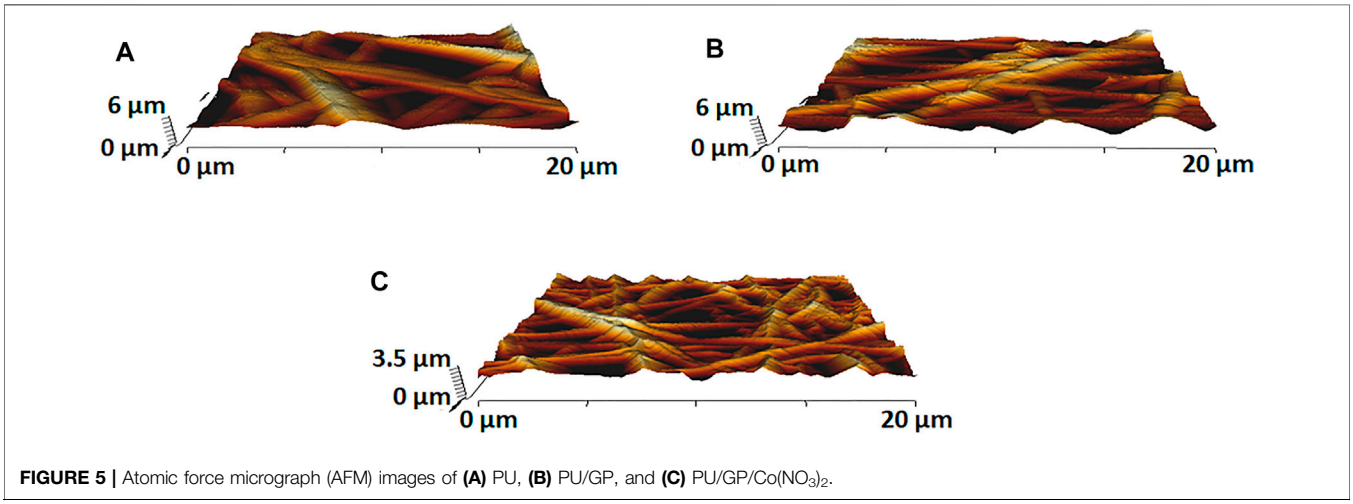

FIGURE 5 | Atomic force micrograph (AFM) images of **(A)** PU, **(B)** PU/GP, and **(C)** PU/GP/$Co(NO_3)_2$.

517°C to 727°C. In the PU/GP curve, the first loss was seen from 224°C to 372°C, the second loss from 372°C to 553°C, and the third loss from 553°C to 783°C, respectively. While in the PU/GP/$Co(NO_3)_2$ weight loss curve, the first loss was seen from 96°C to 354°C, the second loss from 354°C to 497°C, and the third loss from 497°C to 703°C, respectively.

AFM Analysis

AFM was performed to analyze the change in the surface roughness of the polyurethane scaffold while adding GP and $Co(NO_3)_2$, and the representative 3D images are shown in **Figure 5**. The pristine PU showed an average roughness (R_a) of 854 ± 32 nm, while the PU containing GP and GP/$Co(NO_3)_2$ displayed an average roughness of 682 ± 227 nm and 430 ± 198 nm, respectively.

Tensile Measurements

Figure 6 depicts the tensile curves of PU with the addition of GP and $Co(NO_3)_2$. The average tensile strength of PU was 6.16 MPa, while incorporating GP and $Co(NO_3)_2$, it was increased to 9.36 and 16.28 MPa, respectively. Furthermore, **Table 1** presents the average results of elastic modulus, yield strength, and elongation at break for the electrospun scaffolds.

Blood Compatibility Measurements

Blood clotting assays, namely, APTT and PT, were used to measure anticoagulant nature of electrospun PU, GP, and GP/$Co(NO_3)_2$, and the results are presented in **Figure 7A, B**. The developed PU/GP and PU/GP/$Co(NO_3)_2$ showed an APTT time of 195 ± 2 s and 189 ± 4 s, while for PU, it was found to be 176 ± 2 s. Similarly, the developed PU/GP and PU/GP/$Co(NO_3)_2$ showed a PT time of 110 ± 1 s and 107 ± 1 s, respectively, while for PU, it was found to be 94 ± 2 s. The prolonged blood clotting time was due to the presence of GP and $Co(NO_3)_2$. Furthermore, a hemolytic assay was also done to measure the toxicity of fabricated scaffolds with the red blood cells (RBCs). The index of the pristine PU was found to be 2.83%,

TABLE 1 | Average results of elastic modulus, yield strength, and elongation at break for the electrospun scaffolds.

Name	Elastic modulus (MPa)	Yield strength (N)	Elongation at break (%)
PU	5.17	12.479	61.89
PU/grapefruit oil	7.60	10.107	79.66
PU/grapefruit oil/cobalt nitrate	10.57	9.524	92.06

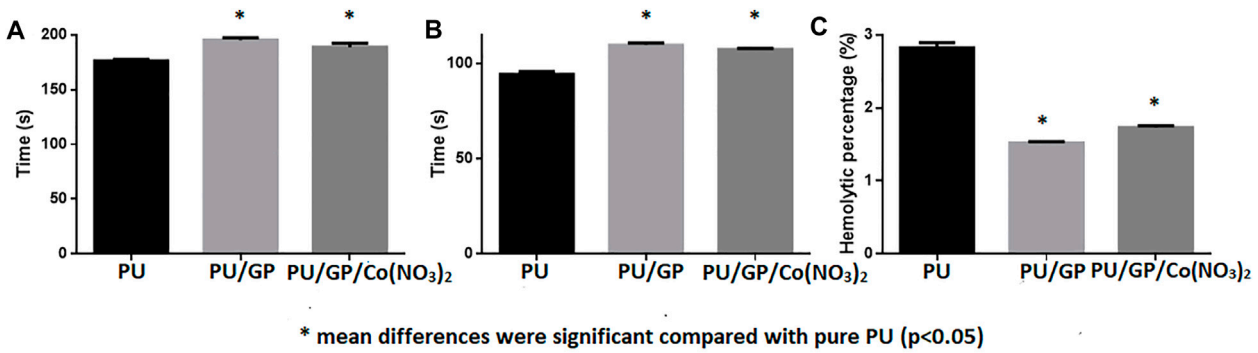

FIGURE 7 | (A) partial thromboplastin time (APTT), **(B)** prothrombin time (PT), and **(C)** hemolytic index of PU, PU/GP, and PU/GP/$Co(NO_3)_2$.

and for PU/GP and PU/GP/$Co(NO_3)_2$ nanocomposite mat, it was calculated to be 1.52% and 1.73%, respectively, as shown in **Figure 7C**.

DISCUSSION

SEM investigation depicted that the addition of GP and $Co(NO_3)_2$ decreased the fiber diameter of the pristine PU. Balaji et al. (2016) electrospun a scaffold based on polyurethane added with honey and papaya. It was shown that the honey and papaya incorporation resulted in the PU fiber diameter. They concluded that this behavior was owing to the bioactive molecules existing in the honey and papaya. Furthermore, they also concluded that this might be due to the changes in the viscosity solution on adding honey and papaya to the PU. Hence, in our study, the reduction in the PU fiber diameter was because of bioactive molecules present in GP. Bioactive molecules might interact with polymeric solution resulting in a change in viscosity of PU solution favoring smaller diameter in composite scaffolds. Lakshman et al. (2010) fabricated a scaffold utilizing a polyurethane scaffold blended with silver nanoparticles using an electrospinning technique. It has been reported that the presence of silver in the PU displayed reduced fiber diameter compared to the control. The reason for this behavior was owing to the increase in the conductivity of the PU solution while adding silver nanoparticles. Hence, in our study, the reduction in the PU fiber diameter was because of both bioactive molecules present in GP and an increase in the conductivity of PU/cobalt nitrate solution. Smaller fiber diameters are reported to have more specific surface area leading to enhanced protein adhesion and cell attachment (Chen et al., 2007). Jaganathan and Mani (2018) fabricated a wound dressing scaffold based on polyurethane added with copper sulfate. The PU fiber diameter was reduced with the addition of copper sulfate, which correlates with our findings. Furthermore, the smaller fibers resulted in the improved adhesion and proliferation of fibroblast cells than the pristine PU. Hence, our electrospun nanocomposites that displayed a smaller fiber diameter might be suitable for wound dressing applications. FTIR analysis showed an increase in peak intensity with the addition of GP and $Co(NO_3)_2$, which was because of the strong hydrogen bond formation (Unnithan et al., 2012). The formation of hydrogen bond was because of the linking of molecules (NH, CH, and CO) present in PU, GP, and $Co(NO_3)_2$. The peak shift and hydrogen bond formation depict the interaction of molecules present in the GP and $Co(NO_3)_2$ within PU matrix. In contact angle measurements, the addition of the GP into the polyurethane matrix had improved its hydrophobicity to an extent, and the change in wettability is due to the constituents present in the GP. Furthermore, the addition of $Co(NO_3)_2$ improved the wettability of the pristine PU. Since the cobalt nitrate contains hydrated water molecules in its structure, this would have inevitably favored the hydrophilic nature of polyurethane. Furthermore, the obtained contact angle results correlate with the FTIR observation, which indicated the formation of broad band of hydroxyl groups at 3,318 cm^{-1} in the spectra of PU/GP/$Co(NO_3)_2$. The increased wettability will enhance the quality of the scaffold in tissue engineering application as this will enable the better distribution in the scaffold during seeding of cells (Yassin et al., 2016). Jaganathan and Mani (2019) electrospun a wound dressing scaffold utilizing polyurethane incorporated with zinc particles. The electrospun PU/zinc nitrate showed a hydrophilic behavior, which correlates with our observation. Furthermore, it displayed enhanced fibroblast cell adhesion than the pristine PU. In this study, the addition of $Co(NO_3)_2$ converts the PU to have a hydrophilic

behavior, which might be suitable for wound dressing applications. TGA was performed at a high temperature in order to predict the scaffold thermal stability, interaction of added constituents, and integrity (Samouillan et al., 2011; Bhugul and Choudhari, 2013; Hassiba et al., 2017). The thermal stability was increased with the reinforcement of GP and decreased while adding cobalt nitrate. Manikandan et al. (2017) electrospun a scaffold based on polyurethane added with murivennai oil nanofibers. The PU/murivennai scaffold showed enhanced thermal behavior, which correlates with the observation of PU/grapefruit oil scaffold. The cobalt nitrate salt contains volatile components (H_2O), which have been evaporated on heating, causing a decrease in the thermal stability of PU/grapefruit oil/cobalt nitrate scaffold (Koohkan et al., 2018). Nirmala et al. (2013) reported the decrease in the thermal stability of the PU with the addition of copper oxide and attributed this behavior to the cations of copper (add reference). Hence, in our study, the cobalt cations might also have a putative role in decreasing the thermal stability. In DTG analysis, the onset and close peaks in the PU/GP and PU/GP/$Co(NO_3)_2$ were different from the pristine polyurethane. This once again corroborates that the added material was integrated into the polyurethane matrix. AFM results clearly depicted that the surface of PE/GP and PE/GP/$Co(NO_3)_2$ was smoother. The change in the roughness behavior was due to the molecules present in GP and $Co(NO_3)_2$. The decrease in the surface roughness might be because of bioactive constituents present in the GP oil. The roughness was reduced further on adding $Co(NO_3)_2$ to PU/GP, which might be due to the interaction of bioactive components in the GP oil with the molecules of the $Co(NO_3)_2$, respectively. Kim et al. (2016) reported a surface roughness analysis in electrospun scaffold utilizing PCL with different diameters. It has been reported that scaffolds with smaller diameter showed smoother surfaces compared to the larger fiber diameter scaffold. Hence, the smoother surfaces of the developed nanocomposite might be because of their smaller fiber diameter of the composite scaffolds. Huag et al. (2009) prepared microporous poly(hydroxybutyric acid) membranes and studied the effect of roughness on osteoblast and fibroblast cell attachment. It has been reported that the membranes with flat surfaces displayed higher fibroblast cell attachment. Hence, both our electrospun composites with smoother surfaces might play an important role in the growth of new tissues. The addition of GP and $Co(NO_3)_2$ enhanced the tensile strength of the pristine PU as revealed in the tensile measurements. Mani et al. (2019) fabricated a scaffold utilizing polyurethane added with magnesium oxide and neem oil. It has been reported that the incorporation of magnesium oxide and neem oil resulted in the enhancement of the tensile strength and concluded that this behavior was because of their smaller fiber diameter. Furthermore, Unnithan et al. (2012) reported that their composite based on polyurethane added with emu oil showed improved tensile strength compared to the pure PU and concluded that this might be because of the hydrogen bond formation between PU and emu oil. The above works favor our hypothesis that the addition of GP oil and cobalt nitrate increased the tensile strength. From the FTIR, the formation of hydrogen bond in our prepared nanocomposites was evident, favoring the increase in mechanical strength. The results of coagulation assays depicted the increase in anticoagulant nature of the electrospun PU/GP and PU/GP/$Co(NO_3)_2$ than the PU scaffold. Furthermore, the fabricated nanocomposite scaffolds showed less toxic to the red blood cells than the pristine PU. Hence, the fabricated composite behaves as a non-hemolytic material according to ASTMF756-00 (2000) (Balaji et al., 2016). The electrospun PU/GP scaffold showed better blood compatibility compared to the pure polyurethane, which may be due to its hydrophobic nature. However, the blood clotting time was slightly reduced while blending $Co(NO_3)_2$ to the PU/GP, and this might be because of change in polar and apolar region (Szycher, 1991). However, their anticoagulation times were higher than the pristine PU. Blood compatibility is a complex phenomenon, and it is influenced by several surface parameters (wettability, fiber diameter, and surface roughness) according to recent research (Huang et al., 2003). Zhou and Yi (1999) developed PU composite membranes added with liquid crystal. The fabricated nanocomposite displayed a hydrophobic nature and enhanced blood clotting time compared to PU. Milleret et al. (2012) used DegraPol and poly lactic-co-glycolic acid (PLGA) polymers for making a scaffold with different fiber diameters. The scaffold with a smaller fiber diameter showed delayed blood clotting. From these literature, it has been observed that the scaffolds with smaller fiber diameter and hydrophobic behavior are conducive for enhanced blood compatibility. The increased blood compatibility of PU/grapefruit oil and PU/grapefruit oil/cobalt nitrate may be attributed to the above surface parameters.

CONCLUSION

A novel combination of electrospun composite comprising GP and $Co(NO_3)_2$ was successfully fabricated through electrospinning. The developed composites PU/GP and PU/GP/$Co(NO_3)_2$ exhibited superior physicochemical and blood-compatible properties. Hence, PU/GP and PU/GP/$Co(NO_3)_2$ composites may serve as potential candidates for scaffolding in tissue engineering applications. However, further testing in both preclinical and clinical setting may anchor the potency of the fabricated composite. A thorough antibacterial investigation and cellular biocompatibility studies of the fabricated membranes should be evaluated to further promote the candidacy of the scaffolds in tissue engineering applications.

DATA AVAILABILITY STATEMENT

The original contributions presented in the study are included in the article/Supplementary Material; further inquiries can be directed to the corresponding author.

AUTHOR CONTRIBUTIONS

Conceptualization: SJ, AM, SM, and AI; methodology: MM and SJ; software: MM, SJ, AM, SM, and AI; validation: MM, SJ, AM, SM, AI, RR, and MA; formal analysis: MM, SJ, AM, SM, AI, RR,

and MA; investigation: MM, SJ, AM, SM, AI, RR, and MA; resources: SJ, AM, SM, and AI; data curation: MM, SJ, AM, SM, AI, RR, and MA; writing—original draft preparation: MM; writing—review and editing: MM, SJ, AM, SM, AI, RR, and MA; visualization: SJ, AM, SM, AI, RR, and MA; supervision: SJ, AM, SM, and AI; project administration: SJ, AM, SM, and AI; funding acquisition: SJ, AM, SM, and AI. All authors contributed to the article and approved the submitted version.

REFERENCES

Ali, I. H., Khalil, I. A., and El-sherbiny, I. M. (2016). Single-Dose Electrospun Nanoparticles-In-Nanofibers Wound Dressings with Enhanced Epithelialization, Collagen Deposition, and Granulation Properties. *ACS Appl. Mater. Inter.* 8, 14453–14469. doi:10.1021/acsami.6b04369

Almasian, A., Najafi, F., Eftekhari, M., Ardekani, M. R. S., Sharifzadeh, M., and Khanavi, M. (2020). Polyurethane/carboxymethylcellulose Nanofibers Containing Malva Sylvestris Extract for Healing Diabetic Wounds: Preparation, Characterization, *In Vitro* and *In Vivo* Studies. *Mater. Sci. Eng. C* 114, 111039. doi:10.1016/j.msec.2020.111039

Balaji, A., Jaganathan, S. K., Ismail, A. F., and Rajasekar, R. (2016). Fabrication and Hemocompatibility Assessment of Novel Polyurethane-Based Bio-Nanofibrous Dressing Loaded with Honey and Carica Papaya Extract for the Management of Burn Injuries. *Int. J. Nanomedicine* 11, 4339–4355. doi:10.2147/IJN.S112265

Bhugul, V. T., and Choudhari, G. N. (2013). Synthesis and Characterization of Polypyrrole-Zinc Oxide Nano Composites by *Ex-Situ* Technique and Study of Their thermal &Electrical Properties. *Int. J. Adv. Res. Innovat.* 2 (12), 159–164.

Chen, M., Patra, P. K., Warner, S. B., and Bhowmick, S. (2007). Role of Fiber Diameter in Adhesion and Proliferation of NIH 3T3 Fibroblast on Electrospun Polycaprolactone Scaffolds. *Tissue Eng.* 13 (3), 579–587. doi:10.1089/ten.2006.0205

Cristóbal-luna, J. M., Alvarez-gonzález, I., Madrigal-bujaidar, E., and Chamorro-cevallos, G. (2018). Grapefruit and its biomedical., Antigenotoxic and Chemopreventive Properties. *Food Chem. Toxicol.* 112, 224–234. doi:10.1016/j.fct.2017.12.038

Cui, W., Zhou, Y., and Chang, J. (2010). Electrospun Nanofibrous Materials for Tissue Engineering and Drug Delivery. *Sci. Tech. Adv. Mater.* 11 (1), 014108. doi:10.1088/1468-6996/11/1/014108

Eltom, A., Zhong, G., and Muhammad, A. (2019). Scaffold Techniques and Designs in Tissue Engineering Functions and Purposes, a Review. *Adv. Mater. Sci. Eng.* 2019, 3429527. doi:10.1155/2019/3429527

Hassiba, A., El Zowalaty, M., Webster, T., Abdullah, A., Nasrallah, G., Khalil, K., et al. (2017). Synthesis, Characterization, and Antimicrobial Properties of Novel Double Layer Nanocomposite Electrospun Fibers for Wound Dressing Applications. *Ijn* 12, 2205–2213. doi:10.2147/ijn.s123417

Hoppe, A., Jokic, B., Janackovic, D., Fey, T., Greil, P., Romeis, S., et al. (2014). Cobalt-releasing 1393 Bioactive Glass-Derived Scaffolds for Bone Tissue Engineering Applications. *ACS Appl. Mater. Inter.* 6 (4), 2865–2877. doi:10.1021/am405354y

Huag, H.-S., Chou, S.-H., Don, T.-M., Lai, W.-C., and Cheng, L.-P. (2009). Formation of Microporous Poly(hydroxybutyric Acid) Membranes for Culture of Osteoblast and Fibroblast. *Polym. Adv. Technol.* 20 (12), 1082–1090. doi:10.1002/pat.1366

Huang, N., Yang, P., Leng, Y. X., Chen, J. Y., Sun, H., Wang, J., et al. (2003). Hemocompatibility of Titanium Oxide Films. *Biomaterials* 24, 2177–2187. doi:10.1016/s0142-9612(03)00046-2

Jaganathan, S. K., and Mani, M. P. (2018). Electrospun Polyurethane Nanofibrous Composite Impregnated with Metallic Copper for Wound-Healing Application. *3 Biotech.* 8 (8), 327. doi:10.1007/s13205-018-1356-2

Jaganathan, S. K., and Mani, M. P. (2019). Single-stage Synthesis of Electrospun Polyurethane Scaffold Impregnated with Zinc Nitrate Nanofibers for Wound Healing Applications. *J. Appl. Polym. Sci.* 136 (3), 46942. doi:10.1002/app.46942

Kim, H. H., Kim, M. J., Ryu, S. J., Ki, C. S., and Park, Y. H. (2016). Effect of Fiber Diameter on Surface Morphology, Mechanical Property, and Cell Behavior of Electrospun Poly(ε-Caprolactone) Mat. *Fibers. Polym.* 17 (7), 1033–1042. doi:10.1007/s12221-016-6350-x

Kim, J. I., Pant, H. R., Sim, H.-J., Lee, K. M., and Kim, C. S. (2014). Electrospun Propolis/polyurethane Composite Nanofibers for Biomedical Applications. *Mater. Sci. Eng. C* 44, 52–57. doi:10.1016/j.msec.2014.07.062

Koohkan, R., Hooshmand, T., Tahriri, M., and Mohebbi-Kalhori, D. (2018). Synthesis, Characterization and *In Vitro* Bioactivity of Mesoporous Copper Silicate Bioactive Glasses. *Ceramics Int.* 44 (2), 2390–2399. doi:10.1016/j.ceramint.2017.10.208

Kuo, Y.-C., Hung, S.-C., and Hsu, S.-h. (2014). The Effect of Elastic Biodegradable Polyurethane Electrospun Nanofibers on the Differentiation of Mesenchymal Stem Cells. *Colloids Surf. B: Biointerfaces* 122, 414–422. doi:10.1016/j.colsurfb.2014.07.017

Lakshman, L. R., Shalumon, K. T., Nair, S. V., Jayakumar, R., and Nair, S. V. (2010). Preparation of Silver Nanoparticles Incorporated Electrospun Polyurethane Nano-Fibrous Mat for Wound Dressing. *J. Macromolecular Sci. A* 47 (10), 1012–1018. doi:10.1080/10601325.2010.508001

Li, X., Wang, C., Yang, S., Liu, P., and Zhang, B. (2018). Electrospun Pcl/mupirocin and Chitosan/lidocaine Hydrochloride Multifunctional Double Layer Nanofibrous Scaffolds for Wound Dressing Applications. *Ijn* 13, 5287–5299. doi:10.2147/ijn.s177256

Liu, H., Ding, X., Zhou, G., Li, P., Wei, X., and Fan, Y. (2013). Electrospinning of Nanofibers for Tissue Engineering Applications. *J. Nanomater.* 2013, 495708. doi:10.1155/2013/495708

Mani, M. P., Jaganathan, S. K., Khudzari, A. Z. M., and Prabhakaran, P. (2019). Development of Advanced Nanostructured Polyurethane Composites Comprising Hybrid Fillers with Enhanced Properties for Regenerative Medicine. *Polym. Test.* 73, 12–20. doi:10.1016/j.polymertesting.2018.11.014

Manikandan, A., Mani, M. P., Jaganathan, S. K., Rajasekar, R., and Jagannath, M. (2017). Formation of Functional Nanofibrous Electrospun Polyurethane and Murivenna Oil with Improved Haemocompatibility for Wound Healing. *Polym. Test.* 61, 106–113. doi:10.1016/j.polymertesting.2017.05.008

Milleret, V., Hefti, T., Hall, H., Vogel, V., and Eberli, D. (2012). Influence of the Fiber Diameter and Surface Roughness of Electrospun Vascular Grafts on Blood Activation. *Acta Biomater.* 8 (12), 4349–4356. doi:10.1016/j.actbio.2012.07.032

Nirmala, R., Jeon, K. S., Lim, B. H., Navamathavan, R., and Kim, H. Y. (2013). Preparation and Characterization of Copper Oxide Particles Incorporated Polyurethane Composite Nanofibers by Electrospinning. *Ceramics Int.* 39 (8), 9651–9658. doi:10.1016/j.ceramint.2013.05.087

Pant, H. R., Pokharel, P., Joshi, M. K., Adhikari, S., Kim, H. J., Park, C. H., et al. (2015). Processing and Characterization of Electrospun Graphene Oxide/polyurethane Composite Nanofibers for Stent Coating. *Chem. Eng. J.* 270, 336–342. doi:10.1016/j.cej.2015.01.105

Polymer (2019). Polymer Properties Database. Available at: https,//polymerdatabase.com/polymer%20classes/Polyurethane%20type.html (Accessed June 4, 2019).

Samouillan, V., Delaunay, F., Dandurand, J., Merbahi, N., Gardou, J.-P., Yousfi, M., et al. (2011). The Use of thermal Techniques for the Characterization and Selection of Natural Biomaterials. *Jfb* 2 (3), 230–248. doi:10.3390/jfb2030230

Shen, Z., Lu, D., Li, Q., Zhang, Z., and Zhu, Y. (20152015). Synthesis and Characterization of Biodegradable Polyurethane for Hypopharyngeal Tissue Engineering. *Biomed. Res. Int.* 2015, 1–11. doi:10.1155/2015/871202

Singh, A., Banerjee, S. L., Dhiman, V., Bhadada, S. K., Sarkar, P., Khamrai, M., et al. (2020). Fabrication of Calcium Hydroxyapatite Incorporated Polyurethane-Graphene Oxide Nanocomposite Porous Scaffolds from Poly (Ethylene Terephthalate) Waste: A green Route toward Bone Tissue Engineering. *Polymer* 195, 122436. doi:10.1016/j.polymer.2020.122436

Subramaniam, R., Mani, M. P., and Jaganathan, S. K. (2018). Fabrication and Testing of Electrospun Polyurethane Blended with Chitosan Nanoparticles for Vascular Graft Applications. *Cardiovasc. Eng. Tech.* 9 (3), 503–513. doi:10.1007/s13239-018-0357-y

Szycher, M. (1991). *High Performance Biomaterials, a Complete Guide to Medical and Pharmaceutical Applications*. Boca Raton: CRC Press.

Teixeira, M. A., Amorim, M. T. P., and Felgueiras, H. P. (2020). Poly (Vinyl Alcohol)-Based Nanofibrous Electrospun Scaffolds for Tissue Engineering Applications. *Polym* 12 (1), 7. doi:10.3390/polym12010007

Tetteh, G., Khan, A. S., Delaine-smith, R. M., Reilly, G. C., and Rehman, I. U. (2014). Electrospun Polyurethane/hydroxyapatite Bioactive Scaffolds for Bone Tissue Engineering: The Role of Solvent and Hydroxyapatite Particles. *J. Mech. Behav. Biomed. Mater.* 39, 95–110. doi:10.1016/j.jmbbm.2014.06.019

Tijing, L. D., Ruelo, M. T. G., Amarjargal, A., Pant, H. R., Park, C.-H., Kim, D. W., et al. (2012). Antibacterial and Superhydrophilic Electrospun Polyurethane Nanocomposite Fibers Containing Tourmaline Nanoparticles. *Chem. Eng. J.* 197, 41–48. doi:10.1016/j.cej.2012.05.005

Unnithan, A. R., Pichiah, P. B. T., Gnanasekaran, G., Seenivasan, K., Barakat, N. A. M., Cha, Y.-S., et al. (2012). Emu Oil-Based Electrospun Nanofibrous Scaffolds for Wound Skin Tissue Engineering. *Colloids Surf. A: Physicochemical Eng. Aspects* 415, 454–460. doi:10.1016/j.colsurfa.2012.09.029

Uysal, B., Sozmen, F., Aktas, O., Oksal, B. S., and Kose, E. O. (2011). Essential Oil Composition and Antibacterial Activity of the Grapefruit (Citrus Paradisi. L) Peel Essential Oils Obtained by Solvent-free Microwave Extraction: Comparison with Hydrodistillation. *Int. J. Food Sci. Technol.* 46 (7), 1455–1461. doi:10.1111/j.1365-2621.2011.02640.x

Vasita, R., and Katti, D. S. (2006). Nanofibers and Their Applications in Tissue Engineering. *Int. J. Nanomedicine* 1 (1), 15–30. doi:10.2147/nano.2006.1.1.15

Wang, X., Ding, B., and Li, B. (2013). Biomimetic Electrospun Nanofibrous Structures for Tissue Engineering. *Mater. Today* 16 (6), 229–241. doi:10.1016/j.mattod.2013.06.005

Yassin, M. A., Leknes, K. N., Sun, Y., Lie, S. A., Finne-Wistrand, A., and Mustafa, K. (2016). Surfactant Tuning of Hydrophilicity of Porous Degradable Copolymer Scaffolds Promotes Cellular Proliferation and Enhances Bone Formation. *J. Biomed. Mater Res. Part A* 104 (8), 2049–2059. doi:10.1002/jbm.a.35741

Zennifer, A., Senthilvelan, P., Sethuraman, S., and Sundaramurthi, D. (2021). Key Advances of Carboxymethyl Cellulose in Tissue Engineering & 3D Bioprinting Applications. *Carbohydr. Polym.* 256, 117561. doi:10.1016/j.carbpol.2020.117561

Zhou, C., and Yi, Z. (1999). Blood-compatibility of Polyurethane/liquid crystal Composite Membranes. *Biomaterials* 20 (22), 2093–2099. doi:10.1016/s0142-9612(99)00080-0

Conflict of Interest: The authors declare that the research was conducted in the absence of any commercial or financial relationships that could be construed as a potential conflict of interest.

Publisher's Note: All claims expressed in this article are solely those of the authors and do not necessarily represent those of their affiliated organizations, or those of the publisher, the editors, and the reviewers. Any product that may be evaluated in this article, or claim that may be made by its manufacturer, is not guaranteed or endorsed by the publisher.